Atom interferometer as a freely falling clock for time-dilation measurements

Albert Roura

German Aerospace Center (DLR) Institute of Quantum Technologies, Ulm

based on Quantum Sci. Technol. 10, 025004 (2025)





Part I

Recent update on the ACES Mission



ACES (Atomic Clock Ensemble in Space)

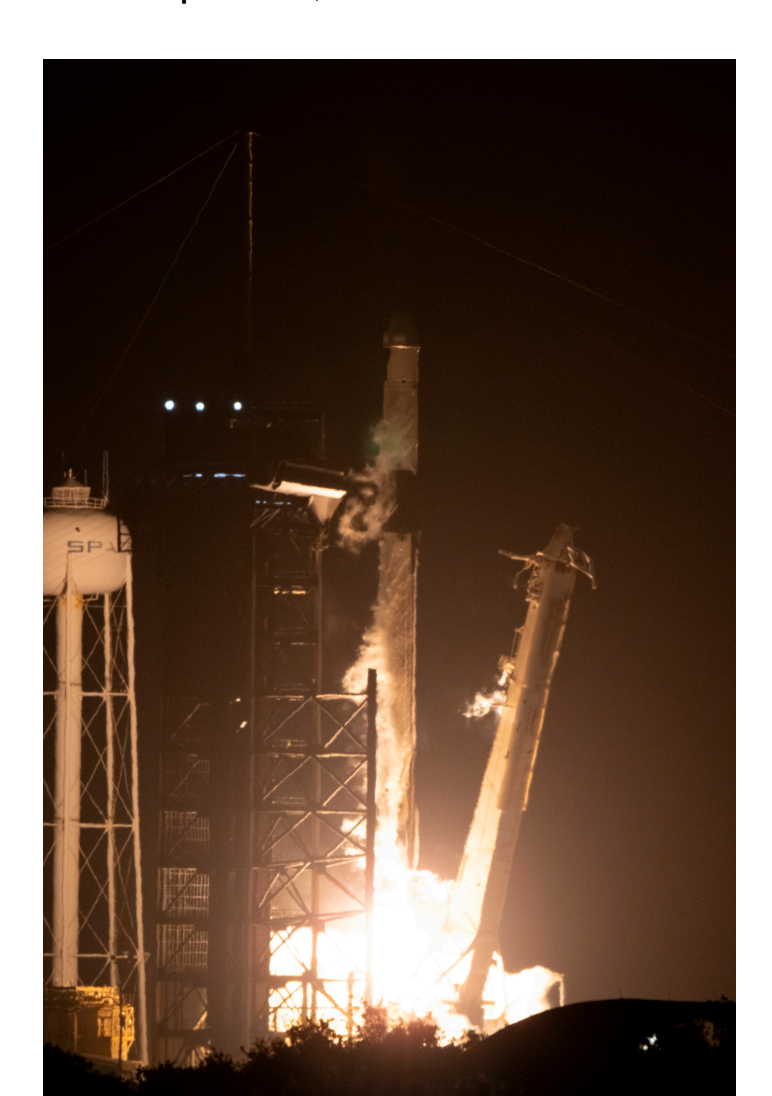


Project scientist: Luigi Cacciapuoti

PI: Christophe Salomon

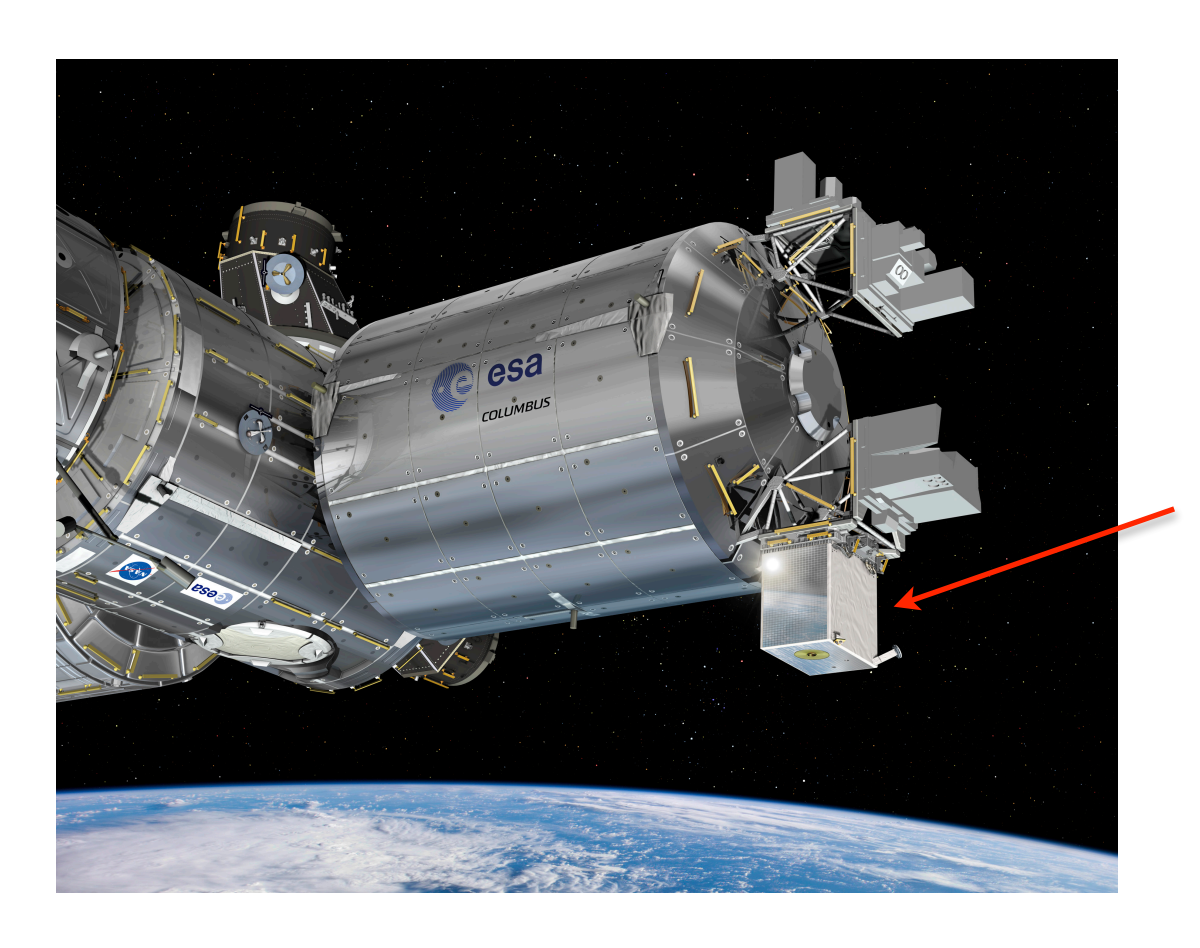
- Target: first high-precision measurements with cold atoms in space.
- Important milestone for future ESA missions with cold atoms.
- Main scientific goals:
 - measuring gravitational redshift at 10^{-6} level
 - searching for dark matter, variations of fundamental constants
 - intercontinental clock comparison at 10⁻¹⁷ level
 - demonstration of chronometric geodesy at 10 cm level

Successful launch on 21 April 2025 Space X, Falcon 9 rocket



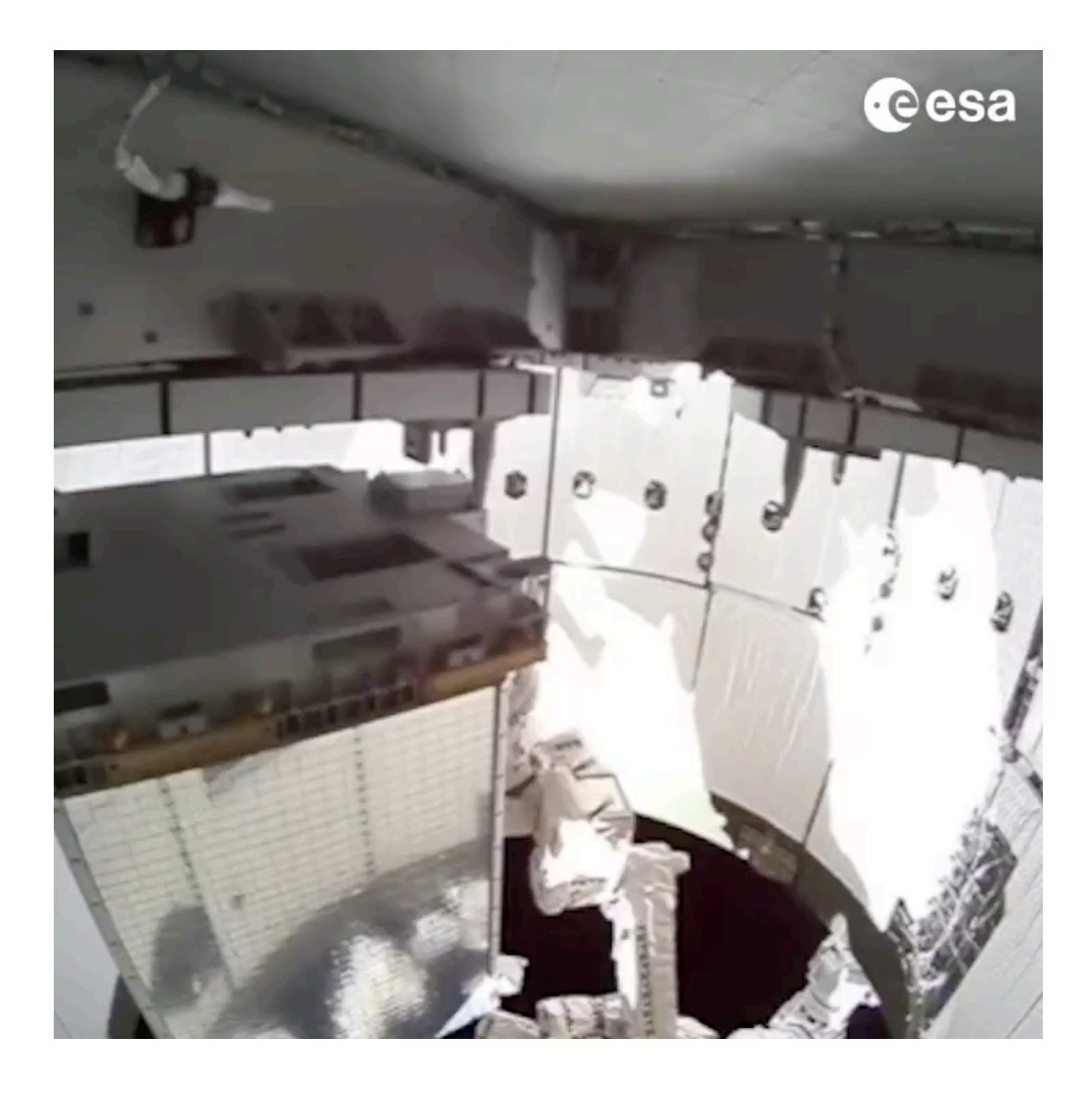


Bartolomeo platform outside the ISS Columbus module



(recording played 100 times faster)





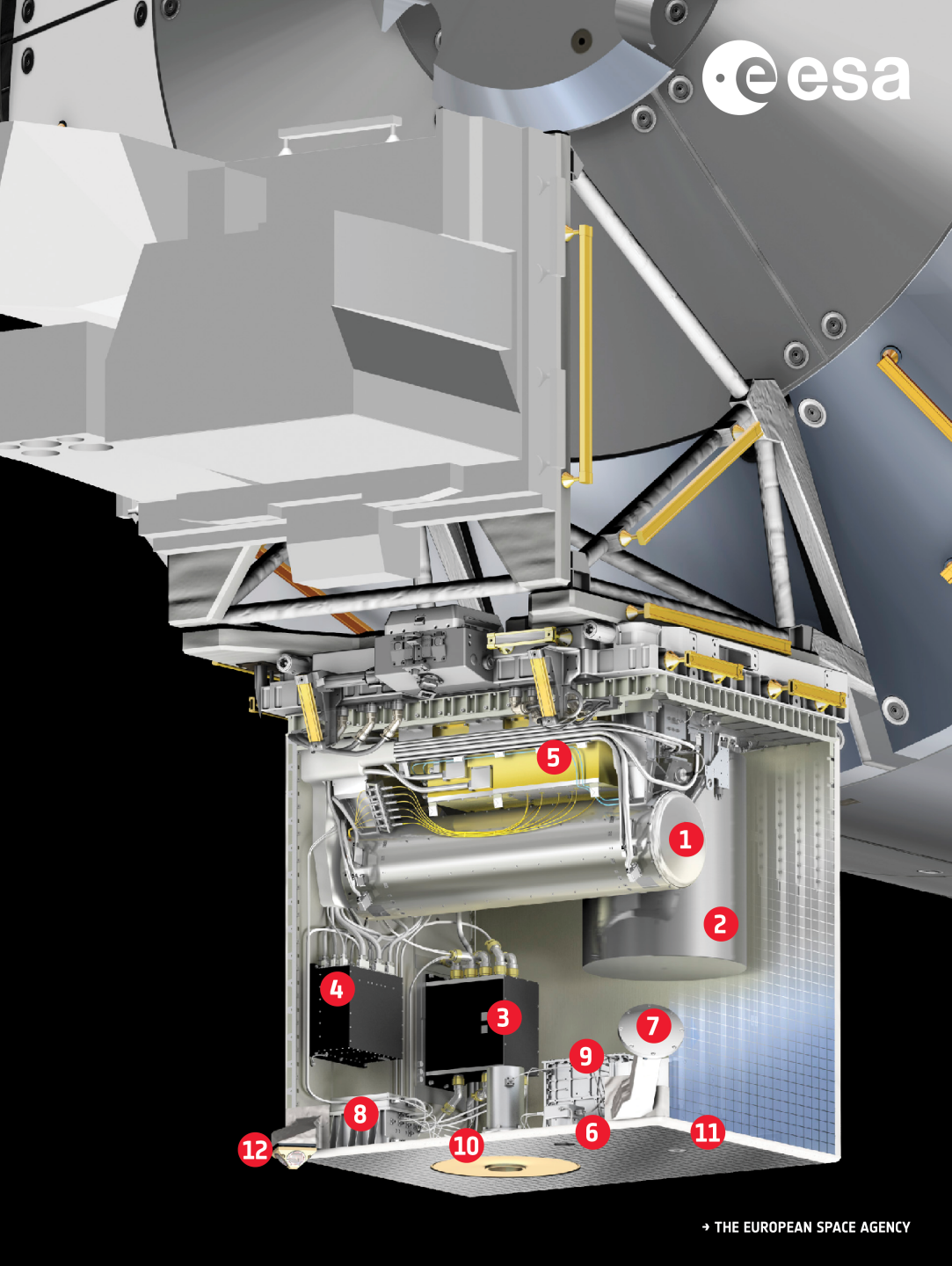
ACES

Atomic Clock Ensemble in Space

A European facility to test fundamental physics from outside ESA's Columbus module on the International Space Station. By creating a "network of clocks", ACES links its own precise timepieces, PHARAO and SHM, with the most accurate clocks on Earth to compare them and measure the flow of time.

- 1 PHARAO
 a clock which uses laser-cooled caesium atoms
- 2) SHM
 Space Hydrogen Maser, a clock which uses hydrogen atoms
- 3 External payload computer (XLPC)
 ACES computer
- 4 PHARAO on-board management unit (OMU)
 PHARAO clock's on-board computer
- 5 PHARAO laser source cools caesium atoms for the PHARAO clock
- 6 Single photon avalanche diode (SPAD)
 a highly sensitive device that can detect single photons of light
- 7 Global navigation satellite system
 (GNSS) antenna
 provides orbit determination of ACES to perform
 fundamental physics tests

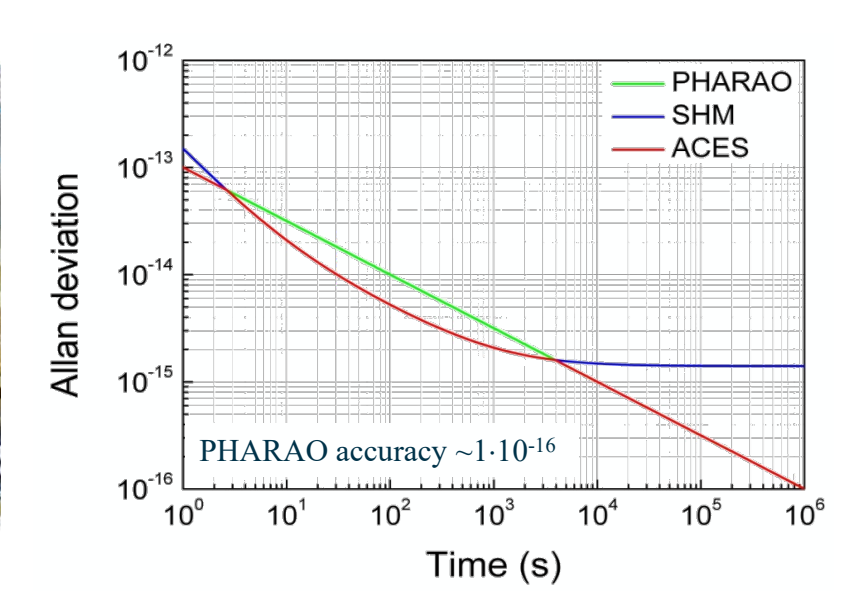
- 8 Frequency comparison and distribution package (FCDP) compares PHARAO and SHM and sends the ACES clock signal to the microwave link electronics
- Microwave link (MWL) enables the comparison of clocks on Earth and in space through the exchange of microwave signals
- 5-band microwave link antenna transmits microwave signals with a frequency of 2.4 GHz, within the 2-4 GHz S-band range used for Wi-Fi and mobile phone communications
- transmits microwave link antenna transmits microwave signals with a frequency of 14.7 GHz a receives signals at a frequency of 13.5 GHz, both within the Ku-band range used mostly for satellite communications
- **European Laser Timing (ELT) reflector**enables the comparison of clocks on Earth and
 in space by using laser pulses



DLR

Highly accurate clock on the ISS:

- Space Hydrogen Maser + Atomic Clock with cold Cs atoms (relative accuracy of 10^{-16}).
- Microwave and Laser links: (intercontinental) comparison of ground clocks at 10^{-17} level.
- First high-precision measurement with cold atoms in space.

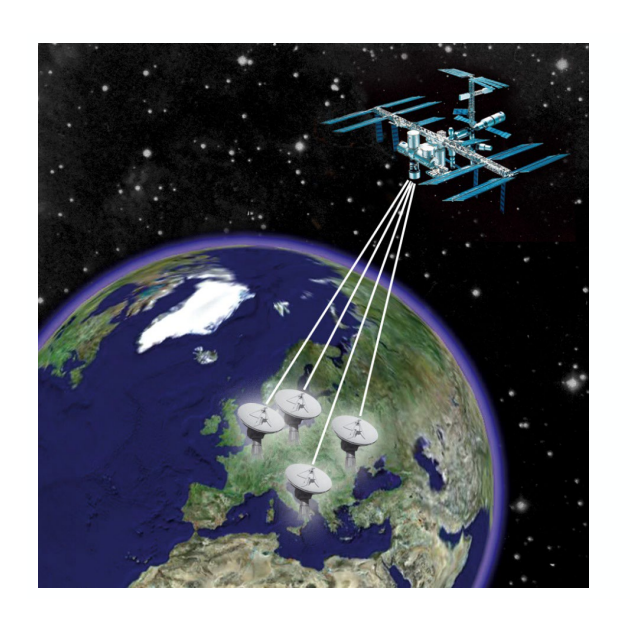


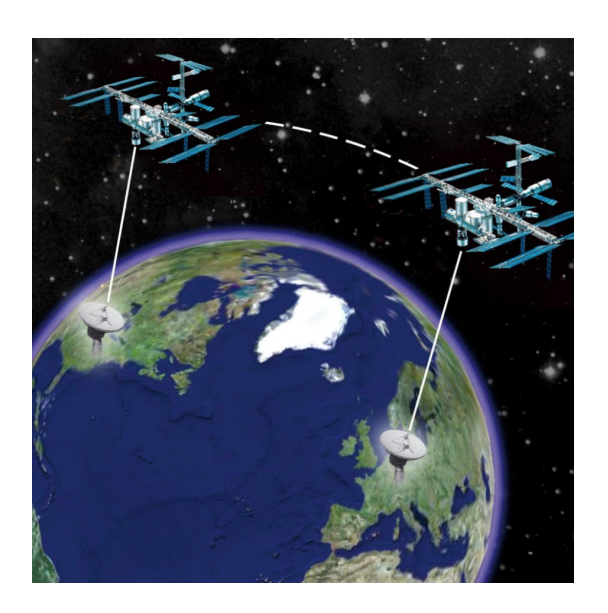




Fundamental Physics measurements:

- Gravitational-redshift (relative uncertainty of 10^{-6}).
- Time variations of fundamental constants.
- Search for topological Dark Matter.

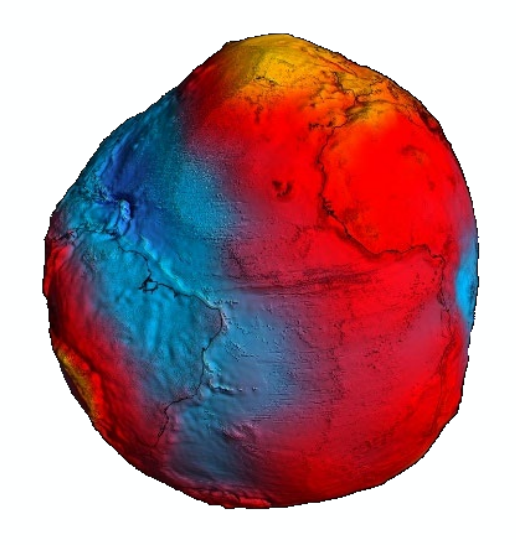


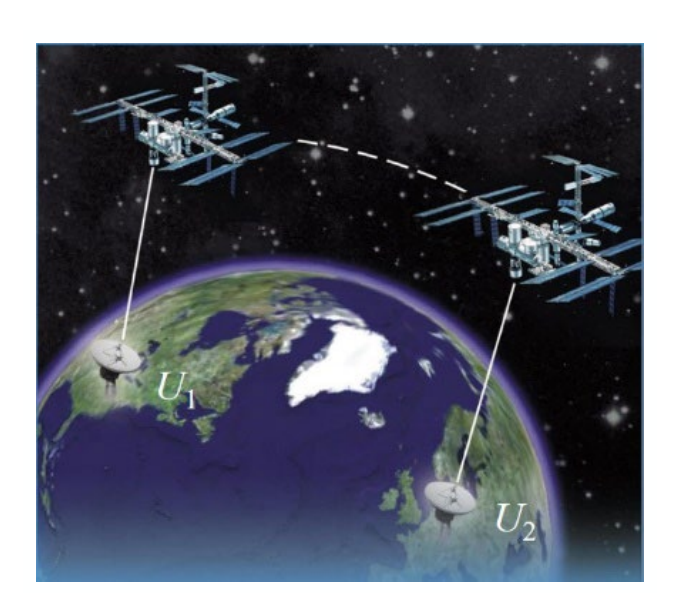


DLR

Other applications:

- Relativistic geodesy (determination of local height above geoid with 10 cm accuracy).
- Clock synchronization at 50 ps level.
- Contribution to atomic time scales (TAI).

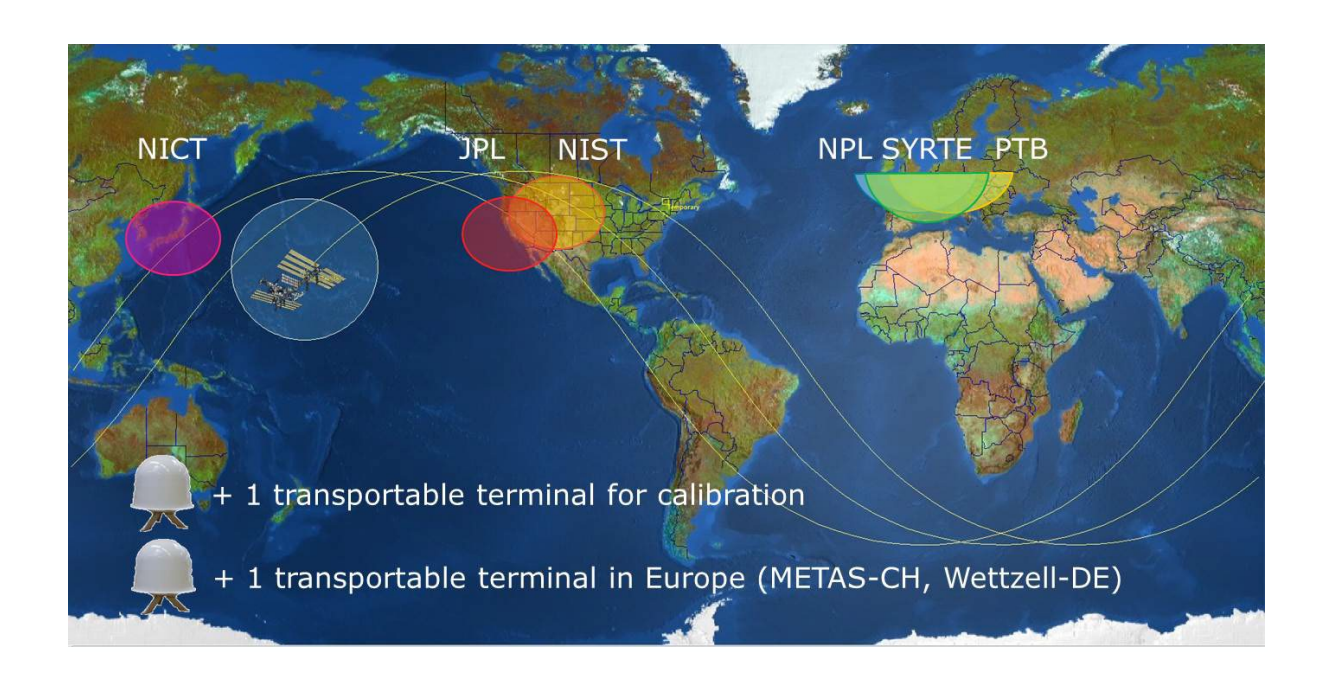






Other applications:

- Relativistic geodesy (determination of local height above geoid with 10 cm accuracy).
- Clock synchronization at 50 ps level.
- Contribution to atomic time scales (TAI).



microwave link (MWL)

participating metrological institutes



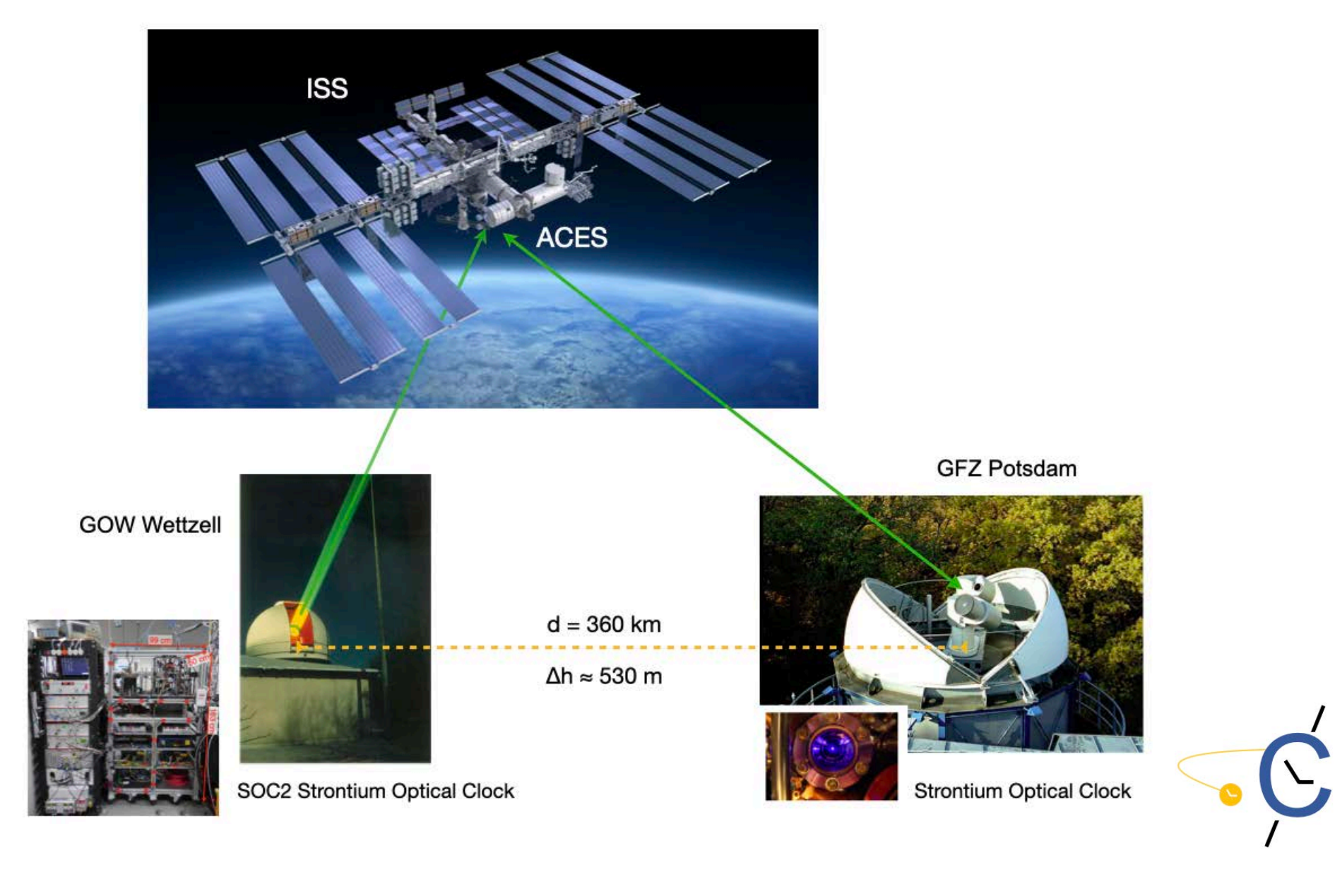
Other applications:

- Relativistic geodesy (determination of local height above geoid with 10 cm accuracy).
- Clock synchronization at 50 ps level.
- Contribution to atomic time scales (TAI).



Satellite Laser Ranging (SLR) stations







Part II

Detection of ultralight dark-matter fields



• Ultralight scalar field as a Dark Matter candidate:

$$\mathcal{L} = +\frac{1}{2}\partial_{\mu}\phi\partial^{\mu}\phi - \frac{1}{2}m_{\phi}^{2}\phi^{2} - \sqrt{4\pi G_{N}}\phi \begin{bmatrix} d_{m_{e}}m_{e}\bar{e}e - \frac{d_{e}}{4}F_{\mu\nu}F^{\mu\nu} \end{bmatrix} + \dots$$

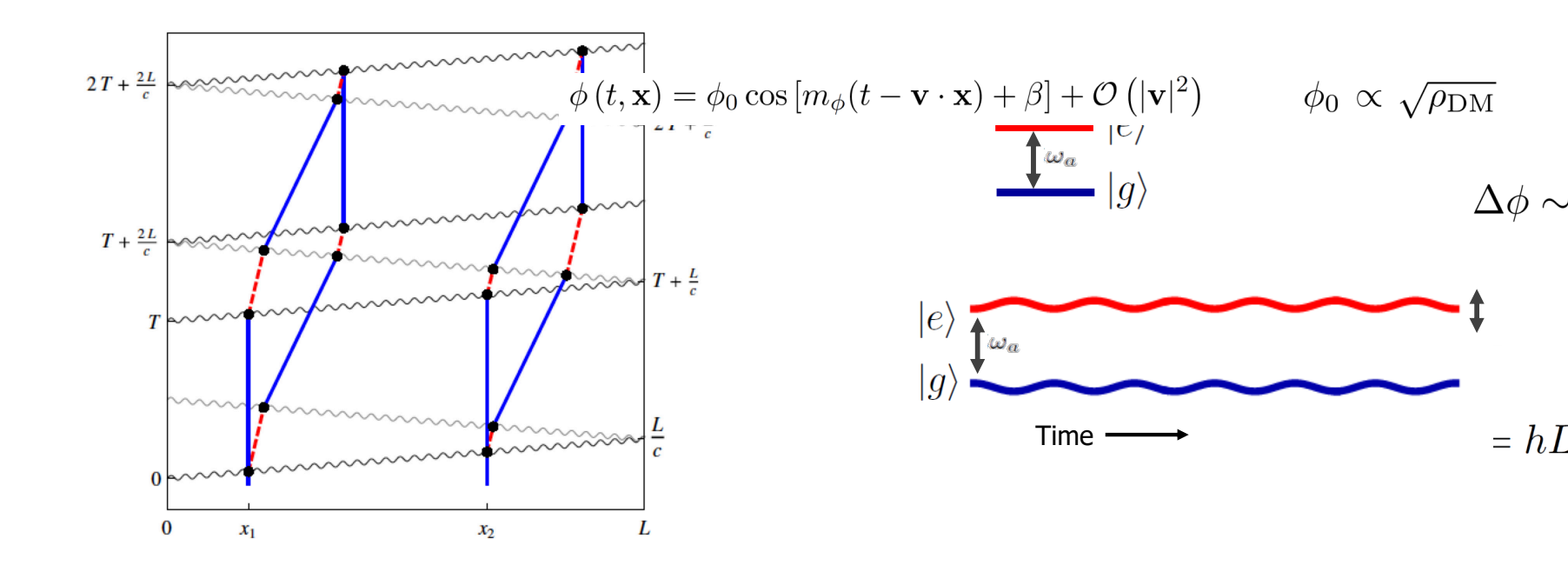
$$\begin{array}{c} \text{Electron} \\ \text{Four coupling} \end{array} \begin{array}{c} \text{Photon} \\ \text{coupling} \end{array} \begin{array}{c} \text{e.g.,} \\ \text{QCD} \end{array}$$

$$\phi\left(t,\mathbf{x}\right) = \phi_{0}\cos\left[m_{\phi}(t-\mathbf{v}\cdot\mathbf{x}) + \beta\right] + \mathcal{O}\left(|\mathbf{v}|^{2}\right) \qquad \phi_{0} \propto \sqrt{\rho_{\mathrm{DM}}} \end{array} \begin{array}{c} \text{DM mass density} \end{array}$$

- Behaving as a bosonic condensate oscillating at the Compton frequency (non-relativistic matter-wave)



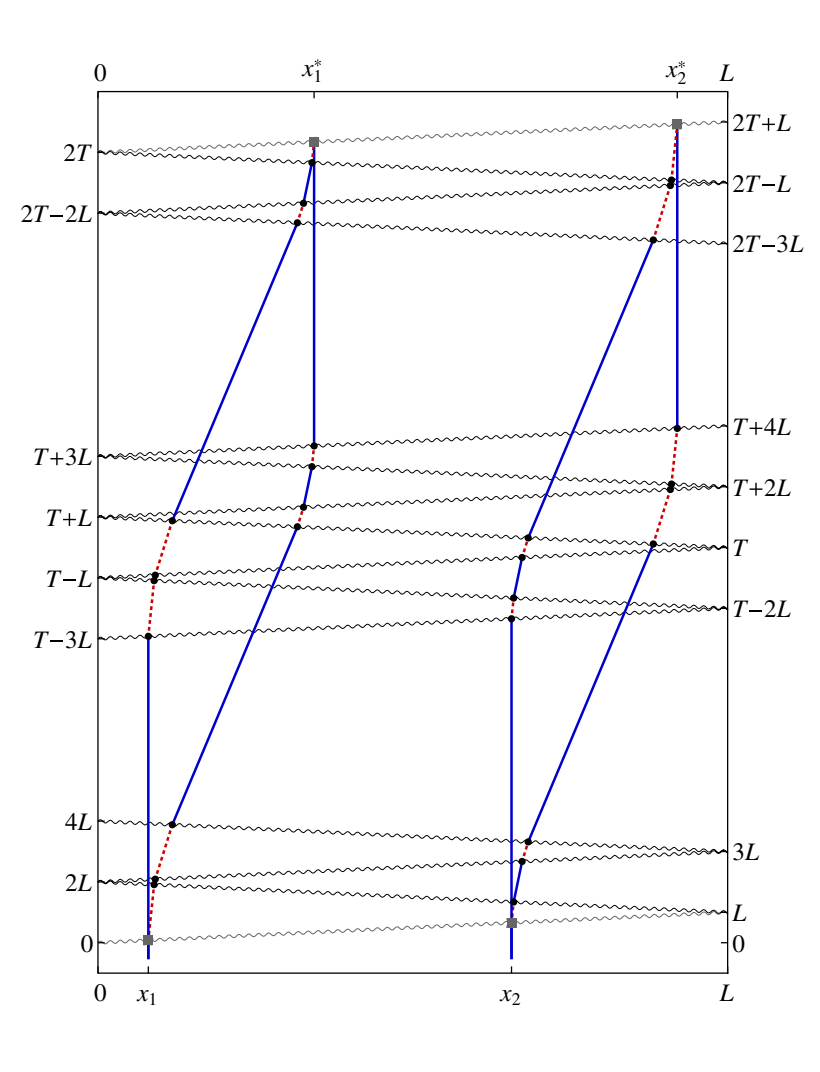
• Oscillations of transition energies at Compton frequency.



• Gradiometry-like differential measurement with atom interferometers based on single-photon diffraction.

• Signal enhancement with LMT pulse sequences:

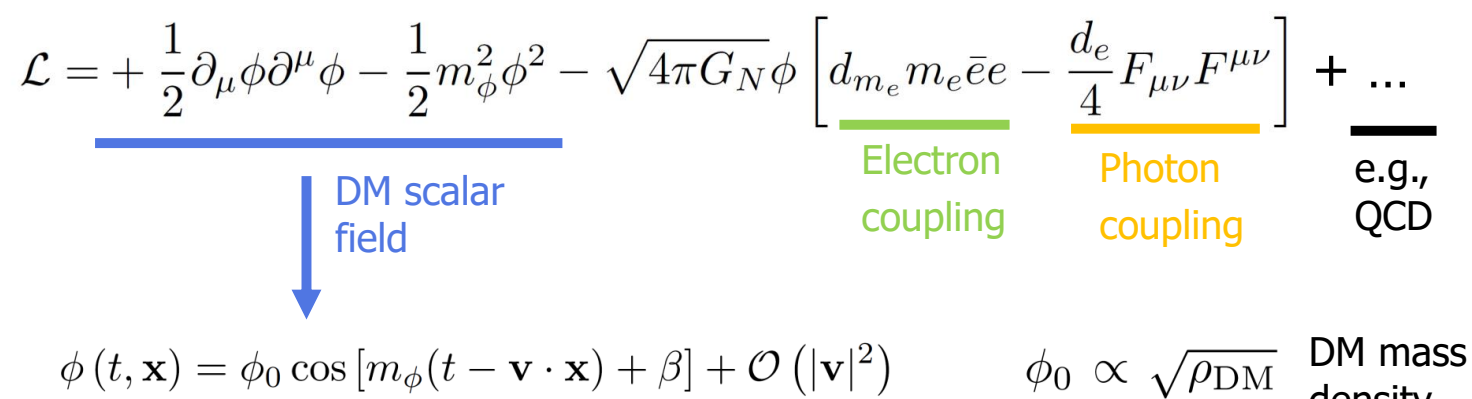


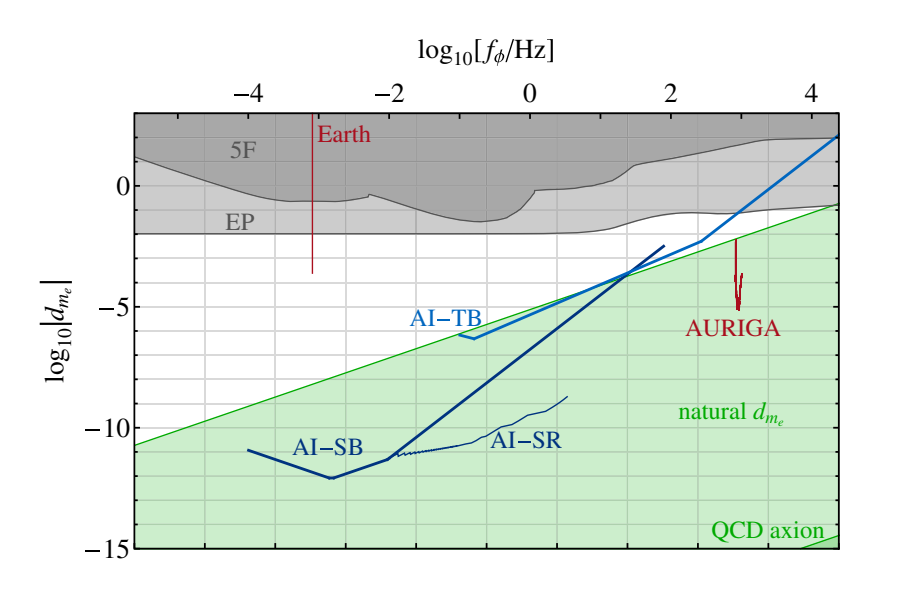


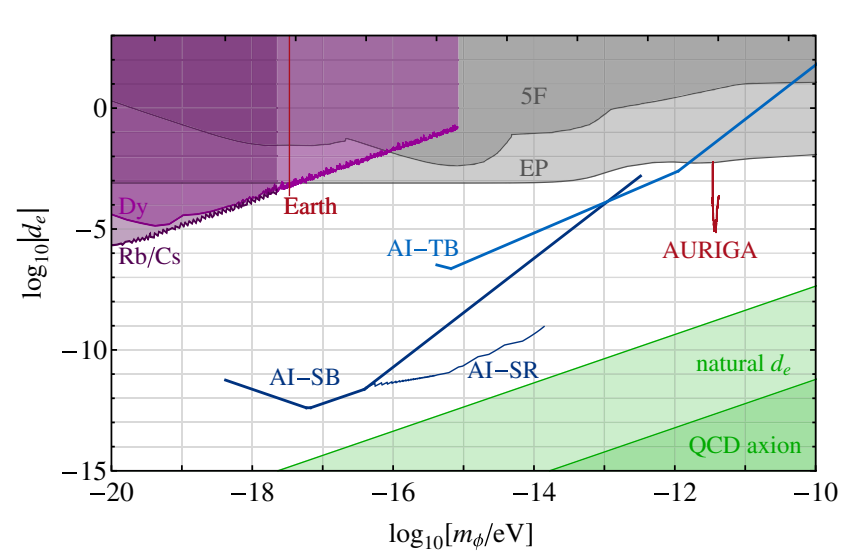
Significant coverage of parameter space:



Arvanitaki et al., Phys. Rev. D **97**, 075020 (2018)



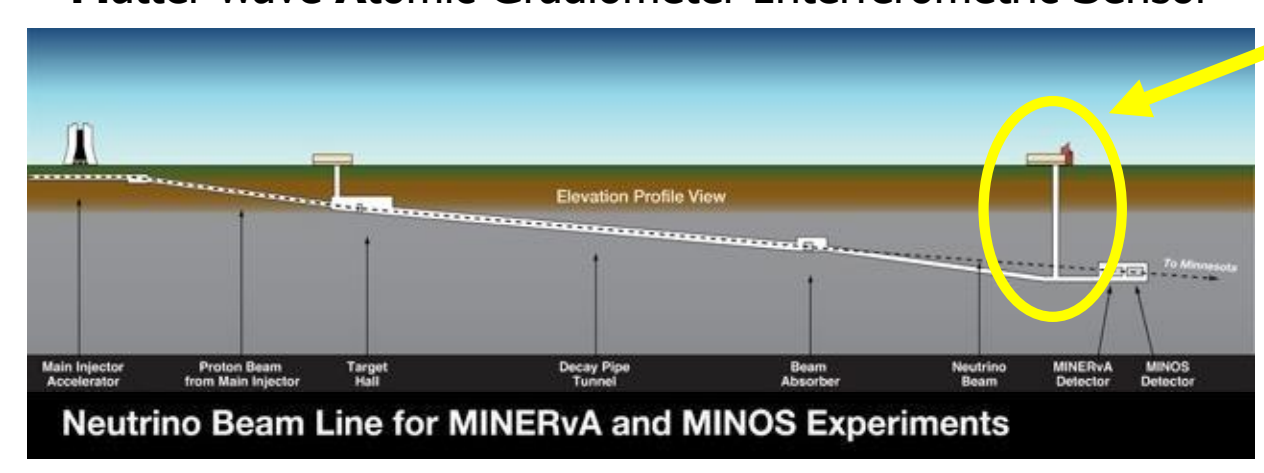




density

MAGIS-100: GW detector prototype at Fermilab





- 100-meter baseline atom interferometry in existing shaft at Fermilab
- Intermediate step to full-scale (km) detector for gravitational waves
- Clock atom sources (Sr) at three positions to realize a gradiometer
- Probes for ultralight scalar dark matter beyond current limits (Hz range)
- Extreme quantum superposition states: >meter wavepacket separation, up to 9 seconds duration















LASER HUTCH

ATOM SOURCE

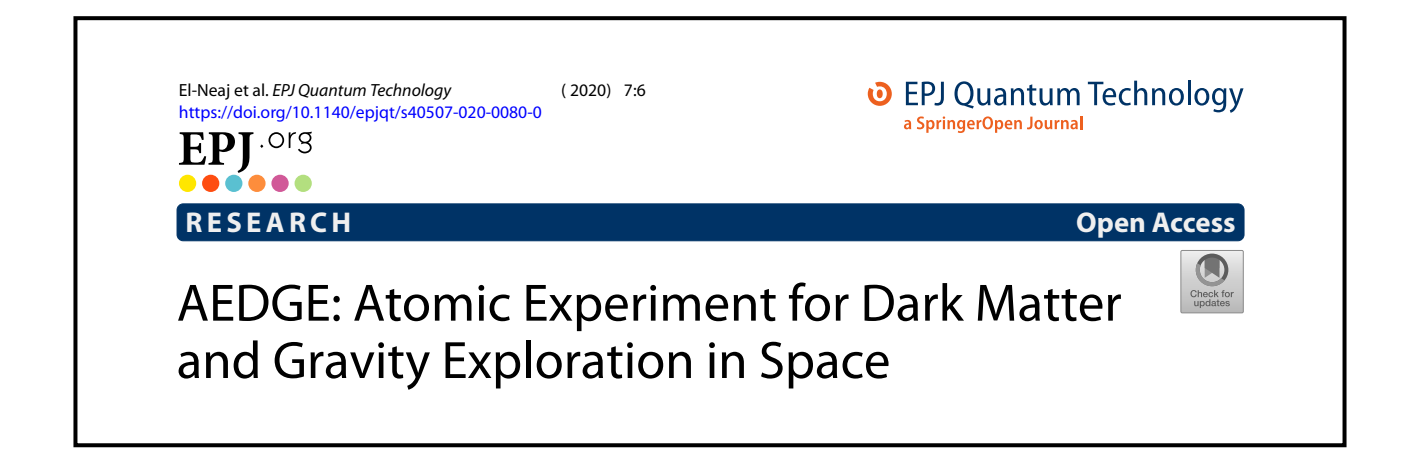
ATOM SOURCE

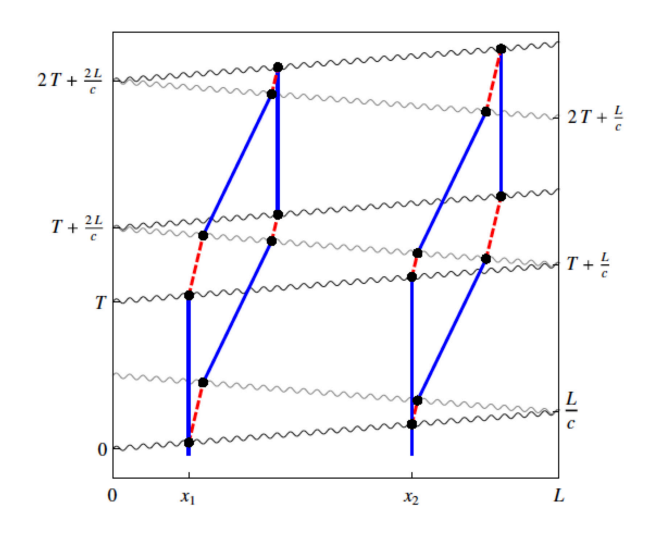
ATOM SOURCE

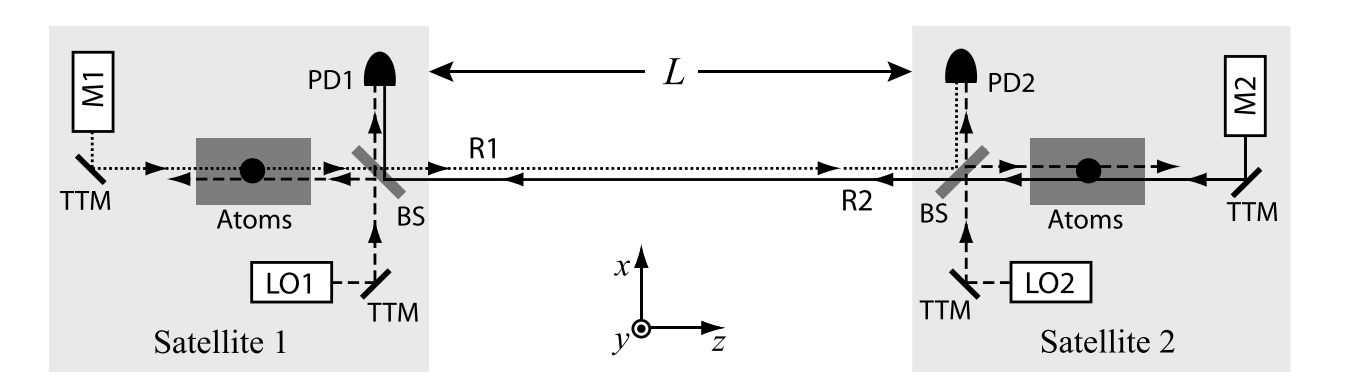
meters

100











Part III

Atom interferometer as a freely falling clock for time-dilation measurements

Motivation



- Applications of atom interferometers based on single-photon transitions:
 - GW detection in mid-frequency band (100-m prototypes not sensitive enough)
 - Search for ultralight dark matter (modest exclusion bounds at early stages)

Are there other interesting measurements (rather than mere null tests) that can be preformed?
 Yes, local measurement of relativistic time dilation with freely falling atoms.

Useful methods for theoretical modelling of such interferometers.

Outline



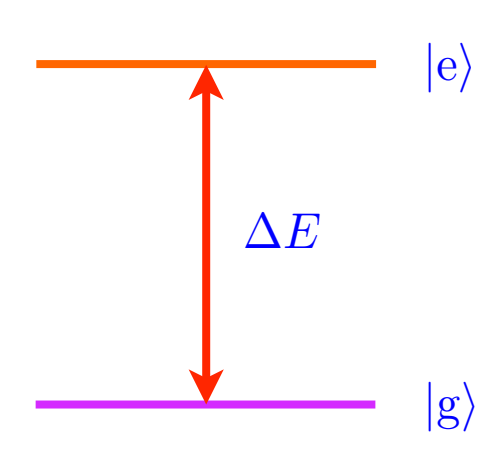
- 1. Relativistic effects in freely falling clocks
- 2. Atom interferometer as a freely falling clock
- 3. Experimental implementation
- 4. Comparison to quantum-clock interferometry
- 5. Conclusions



Relativistic effects in freely falling clocks







• *Initialization* pulse:

$$|\mathbf{g}\rangle \rightarrow |\Phi(0)\rangle = \frac{1}{\sqrt{2}} (|\mathbf{g}\rangle + i e^{i\varphi} |\mathbf{e}\rangle)$$

Evolution:

$$|\Phi(\tau)\rangle \propto \frac{1}{\sqrt{2}} (|\mathbf{g}\rangle + i e^{i\varphi} e^{-i\Delta E \, \tau/\hbar} |\mathbf{e}\rangle)$$



Theoretical description of the clock:

two-level atom (internal state):

$$\hat{H} = \hat{H}_1 \otimes |\mathbf{g}\rangle\langle\mathbf{g}| + \hat{H}_2 \otimes |\mathbf{e}\rangle\langle\mathbf{e}|$$

$$m_1 = m_{\rm g}$$

 $m_2 = m_{\rm g} + \Delta m$
 $\Delta m = \Delta E/c^2$

classical action for COM motion:

$$S_n[x^{\mu}(\lambda)] = -m_n c^2 \int d\tau = -m_n c \int d\lambda \sqrt{-g_{\mu\nu}} \frac{dx^{\mu}}{d\lambda} \frac{dx^{\nu}}{d\lambda} \qquad (n = 1, 2)$$

free fall



Theoretical description of the clock:

two-level atom (internal state):

$$\hat{H} = \hat{H}_1 \otimes |g\rangle\langle g| + \hat{H}_2 \otimes |e\rangle\langle e|$$

$$m_1 = m_{\rm g}$$

 $m_2 = m_{\rm g} + \Delta m$
 $\Delta m = \Delta E/c^2$

classical action for COM motion:

$$S_n[x^{\mu}(\lambda)] = -m_n c^2 \int d\tau \approx \int_{t_0}^t dt' \left(-m_n c^2 + \frac{1}{2} m_n \dot{\mathbf{x}}^2 - m_n U(t', \mathbf{x}) \right)$$

free fall



Propagation of matter-wave packets in curved spacetime (relativistic description)

- Wave-packet evolution in terms of
 - central trajectory (satisfies classical e.o.m.) $X^{\mu}(\lambda)$
 - centered wave packet $\left|\psi_{\mathrm{c}}^{(n)}(au_{\mathrm{c}})\right>$

$$\Delta p/m \ll c$$
 $\Delta x \ll \ell$ curvature radius

For further details:



PHYSICAL REVIEW X 10, 021014 (2020)

Gravitational Redshift in Quantum-Clock Interferometry

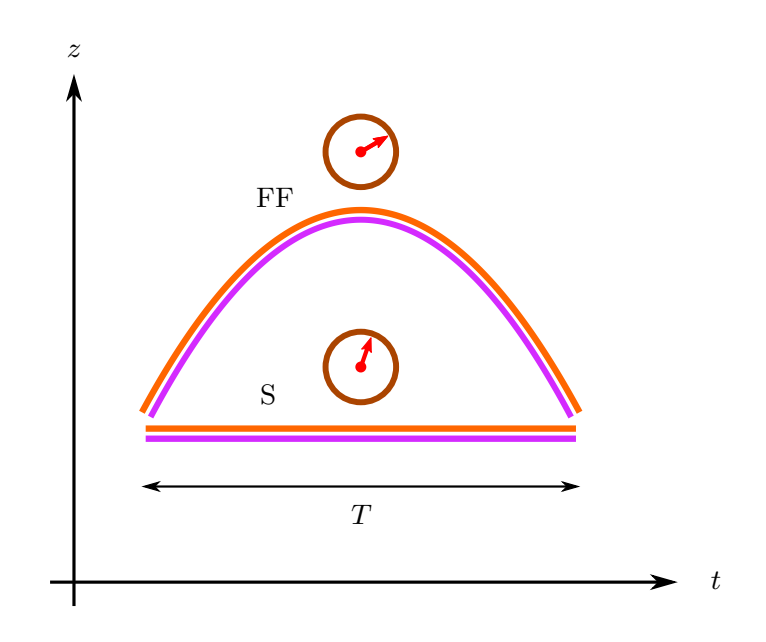
Albert Roura

Institute of Quantum Technologies, German Aerospace Center (DLR), Söflinger Straße 100, 89077 Ulm, Germany and Institut für Quantenphysik, Universität Ulm, Albert-Einstein-Allee 11, 89081 Ulm, Germany

- Relativistic description of atom interferometry in curved spacetime.
- Including external forces and even guiding potentials.
- Relativistic interpretation of the separation phase in open interferometers.

Relativistic time dilation for a freely falling clock





Freely falling clock (FF):

$$\delta \phi = -(\Delta E/\hbar) \left(\left(1 + U_0/c^2 \right) T + \frac{1}{24} \frac{g^2 T^3}{c^2} \right)$$

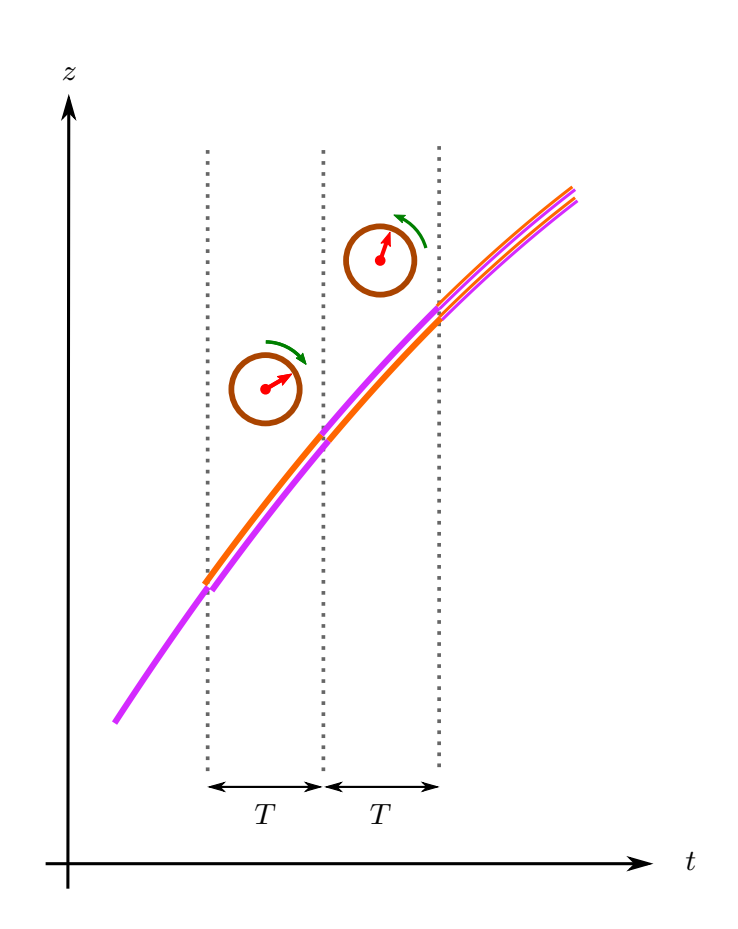
Static clock at constant height (S):

$$\delta\phi = -(\Delta E/\hbar) \left(1 + U_0/c^2\right) T$$

- Natural implementation: compare atomic fountain clock to optical lattice clock.
- BUT accuracy of best atomic fountain clocks insufficient by more than an order of magnitude.







- Simultaneity hypersurfaces in the lab frame.
 (equal time separation)
- Unbalanced proper times (before and after inversion)
 due to relativistic time dilation:

$$\delta \phi = -2 \left(\Delta E / \hbar \right) \left(\mathbf{v}_0 \cdot \mathbf{g} \, T^2 + g^2 T^3 \right) / c^2$$

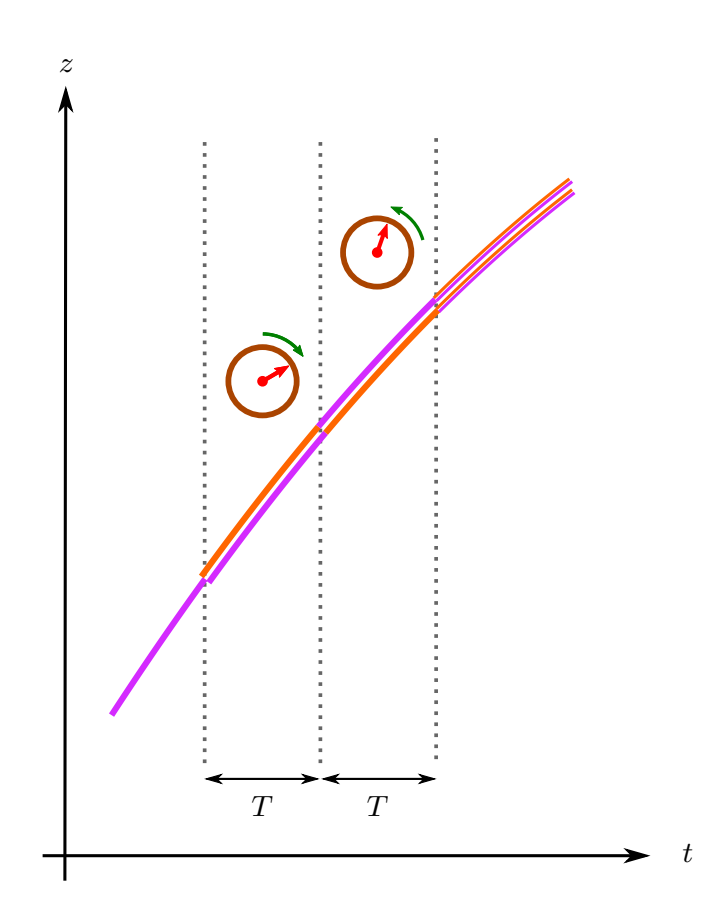
$$\frac{d\tau}{dt} = 1 - \frac{1}{2c^2} \left(\frac{d\mathbf{X}}{dt}\right)^2 + \frac{1}{c^2} U(t, \mathbf{X})$$
and the latitude is a superior of the state of

special relativistic

gravitational redshift







- Possible implementation with *Doppler-free* E2–M1 *two-photon* pulses at $\lambda_2 = 2 \times 698 \, \mathrm{nm}$.
- Drawbacks:
 - dedicated high-power laser needed at λ_2
 - residual recoil ($m \Delta \mathbf{v} = -\Delta m \mathbf{v}$)
- Let us consider atom interferometers based on single-photon transitions.



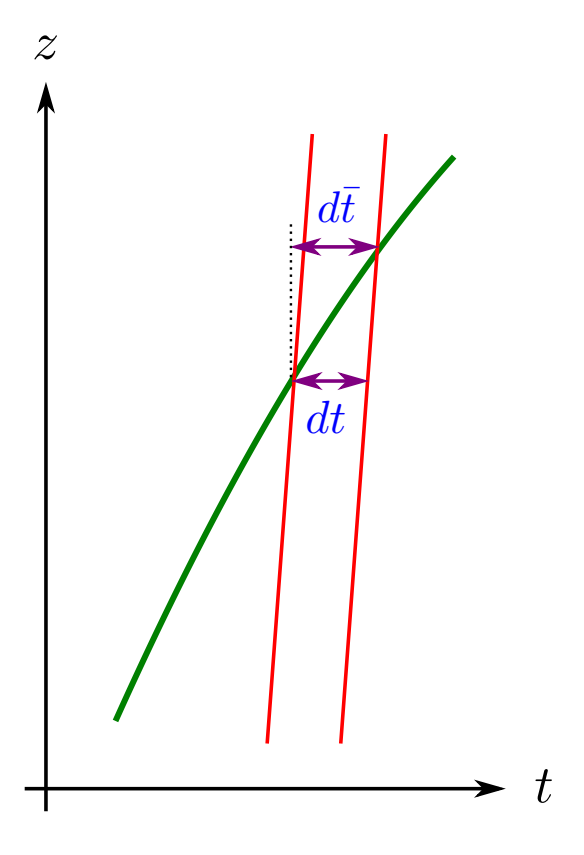
Atom interferometer as a freely falling clock





- Proper time along a freely falling world line (geodesic) and elapsed between two light rays.
 - Retardation effect due to the finite speed of light:

$$d\bar{t} = dt + (\hat{\mathbf{n}} \cdot \bar{\mathbf{v}}/c) d\bar{t} + O(1/c^3)$$







- Proper time along a freely falling world line (geodesic) and elapsed between two light rays.
 - Retardation effect due to the finite speed of light:

(stationary spacetime)

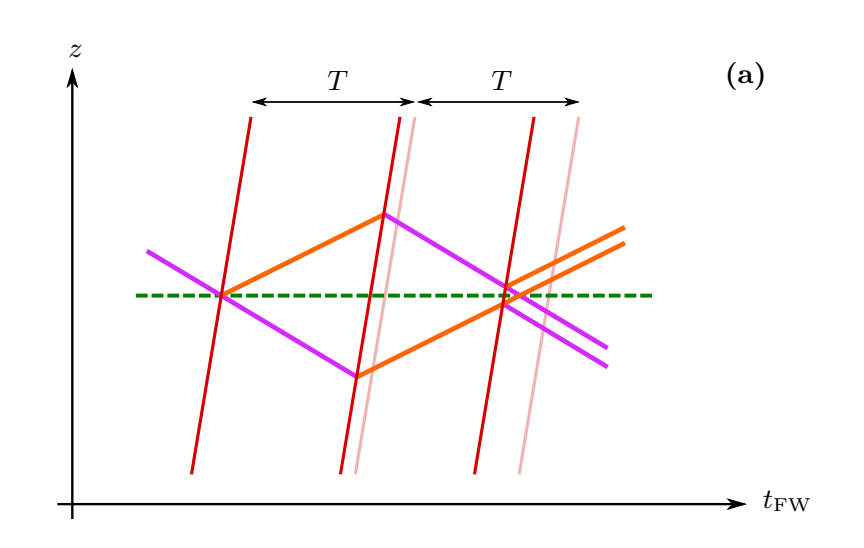
$$d\bar{t} = dt + (\hat{\mathbf{n}} \cdot \bar{\mathbf{v}}/c) d\bar{t} + O(1/c^3) \qquad \longrightarrow \qquad \frac{dt}{dt} = \frac{1}{1 - \hat{\mathbf{n}} \cdot \bar{\mathbf{v}}/c}$$

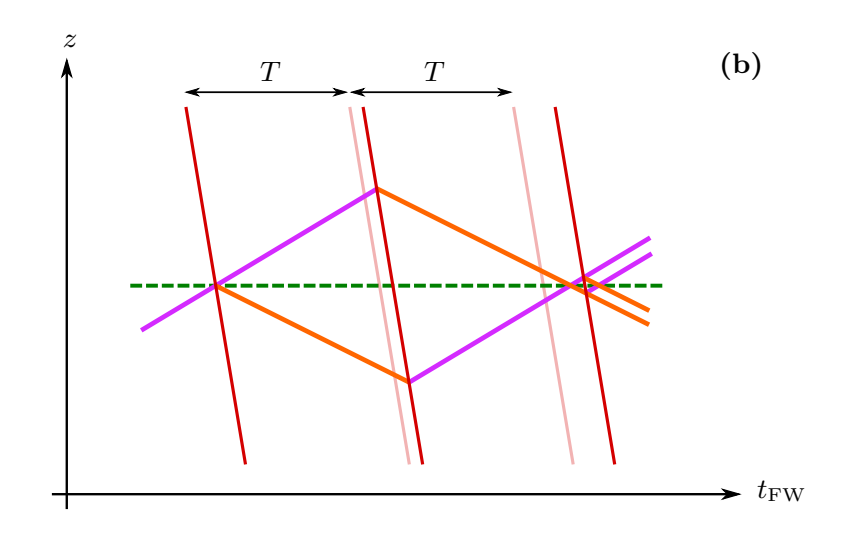
Relativistic time dilation:

$$\frac{d\bar{\tau}}{d\bar{t}} = 1 - \frac{1}{2c^2} \left(\frac{d\bar{\mathbf{X}}}{d\bar{t}}\right)^2 + \frac{1}{c^2} U(\bar{t}, \bar{\mathbf{X}}) + O(1/c^4)$$
 special relativistic gravitational redshift









- Freely falling frame comoving with the mid-point world line (Fermi-Walker frame):
 - light rays (laser wave fronts) have fixed slope,
 - ▶ shifts due to Doppler effect (*opposite sign* in reversed interferometer) and time dilation (*same sign*).



- It is sufficient to calculate the proper times along the mid-point world line rather than the actual arm trajectories (negligible higher-order corrections to total phase shift).
- Proper time as a function of the phase φ , invariant characterizing each laser wave front:

$$\frac{d\bar{\tau}}{d\varphi} = \frac{d\bar{\tau}}{d\bar{t}} \frac{d\bar{t}}{dt} \left(\frac{dt}{d\varphi} \right) = \frac{d\bar{\tau}}{d\bar{t}} \left(\frac{1}{1 - \hat{\mathbf{n}} \cdot \bar{\mathbf{v}}/c} \right) \left(\frac{dt}{d\varphi} \right)$$

The Doppler factor can be (partially) compensated through a suitable frequency chirp:

$$\left(\frac{dt}{d\varphi}\right)_{\text{chirp}} = \left(1 - \hat{\mathbf{n}} \cdot \bar{\mathbf{v}}'/c\right) \left(\frac{dt}{d\varphi}\right)_0 \qquad (dt/d\varphi)_0 = 1/\omega_0$$

$$\bar{\mathbf{v}}'(\bar{t}) = \bar{\mathbf{v}}_0' + \mathbf{g}'(\bar{t} - \bar{t}_0)$$



Phase-shift calculation:

$$\delta \phi = -\frac{\Delta E}{\hbar} \left[\int_0^{\omega_0 T} \left(\frac{d\bar{\tau}}{d\varphi} \right) d\varphi - \int_{\omega_0 T}^{2\omega_0 T} \left(\frac{d\bar{\tau}}{d\varphi} \right) d\varphi \right]$$

■ For an approximately uniform gravitational field, $\bar{\mathbf{X}}(\bar{t}) = \bar{\mathbf{v}}_0 + \mathbf{g}(\bar{t} - \bar{t}_0)$ and

$$\delta \phi = -2 \left(\Delta E / \hbar \right) \left(\bar{\mathbf{v}}_0 \cdot \mathbf{g} \, T^2 + g^2 T^3 \right) / c^2 + \delta \phi_{\text{corr}}$$

• It agrees with the result for an ideal freely falling clock if $\delta\phi_{\rm corr}$ can be kept small enough.



■ For an imperfect match of the chirped frequency, with $\Delta \mathbf{g} = \mathbf{g} - \mathbf{g}'$ and $\Delta \bar{\mathbf{v}}_0 = \bar{\mathbf{v}}_0 - \bar{\mathbf{v}}_0'$.

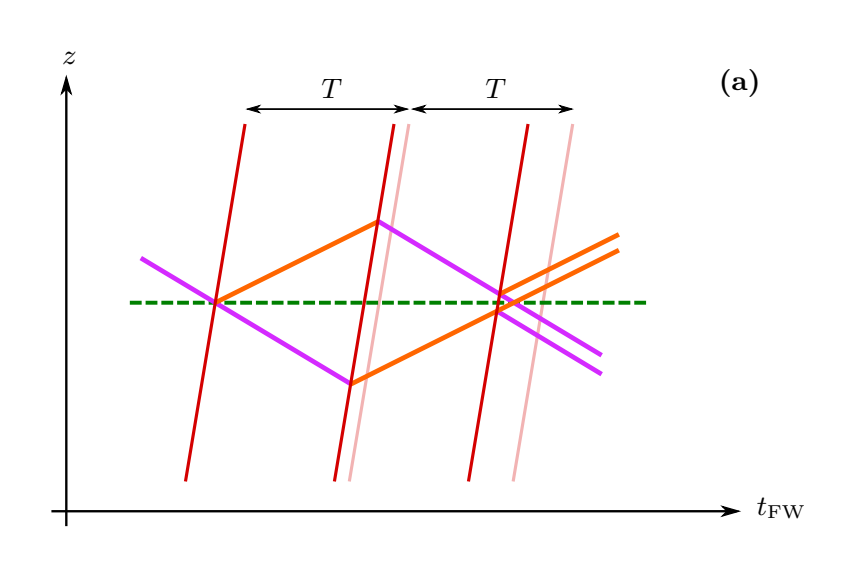
$$\delta\phi_{\text{corr}} = \frac{\Delta E}{\hbar} \left[\frac{(\hat{\mathbf{n}} \cdot \Delta \mathbf{g})}{c} T^2 + 2 \frac{(\hat{\mathbf{n}} \cdot \Delta \bar{\mathbf{v}}_0) (\hat{\mathbf{n}} \cdot \mathbf{g})}{c^2} T^2 + \frac{(\hat{\mathbf{n}} \cdot \bar{\mathbf{v}}_0) (\hat{\mathbf{n}} \cdot \Delta \mathbf{g})}{c^2} T^2 + 3 \frac{(\hat{\mathbf{n}} \cdot \mathbf{g}) (\hat{\mathbf{n}} \cdot \Delta \mathbf{g})}{c^2} T^3 \right]$$

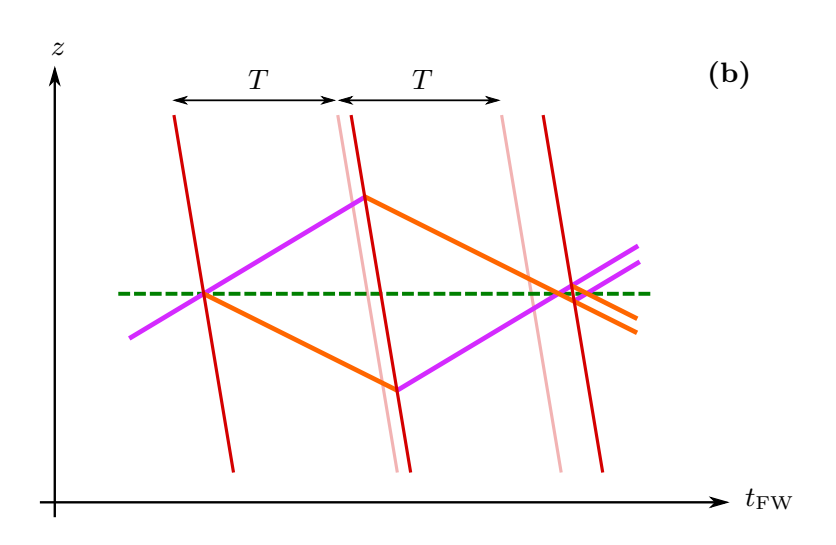
- The dominant term is linear in $\hat{\bf n}$ and can be suppressed by adding up $\delta\phi$ for two interferometers with opposite $\hat{\bf n}$. (reversed interferometers)
- The above result can be straightforwardly generalized to a time dependent $\Delta \mathbf{g}(\bar{t})$.

 This can naturally account for *laser phase noise* and *vibrations* of retro-reflection *mirror*.

Reversed interferometers



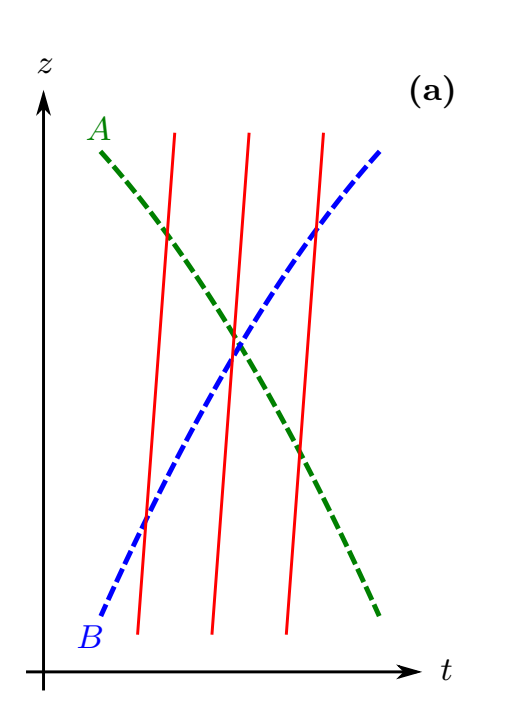


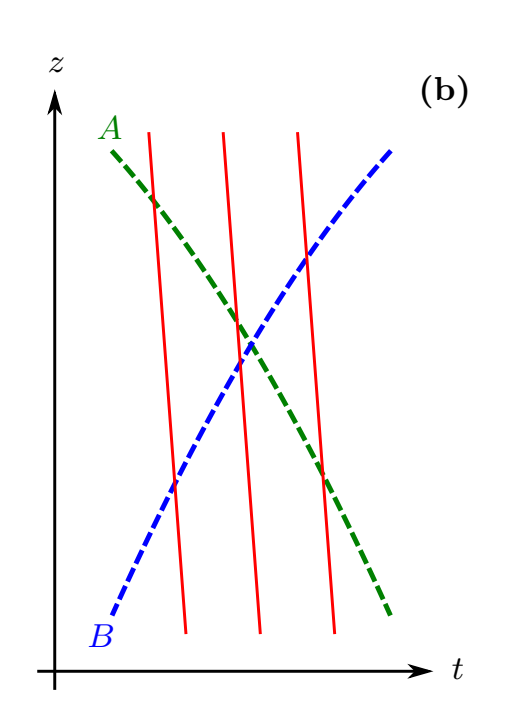


- Uncompensated Doppler contribution cancels out when adding up their phase shifts.
- Effects of *mirror vibrations* and *laser phase noise* (for reversed interferometers in different shots) do not cancel out → "gradiometric" configuration.

"Gradiometric" configuration







Differential phase shift between interferometers
 launched with different velocities (A and B):

$$\delta\phi_A - \delta\phi_B = -2\left(\Delta E/\hbar\right)\left(\bar{\mathbf{v}}_0^A - \bar{\mathbf{v}}_0^B\right) \cdot \mathbf{g} \, T^2/c^2$$

Similarly for pair of reversed interferometers:(a) and (b)

Comparison between two freely falling clocks.
 (no need for highly stable time reference in lab frame)



Experimental implementation



 Gradiometric configuration in MAGIS-100 with two simultaneous interferometers launched from the top and bottom atom source.

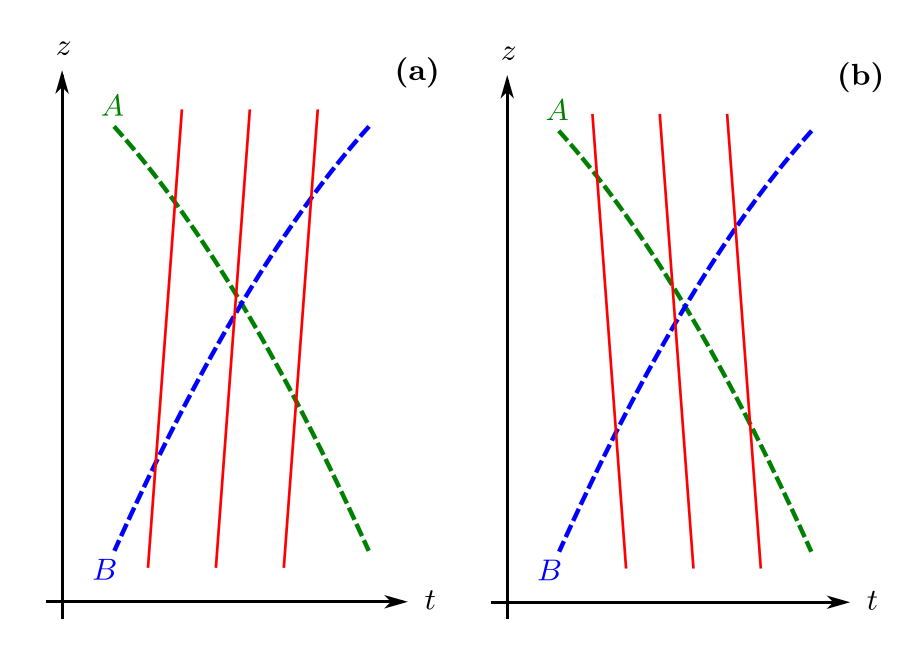
AOM driven by a stable rf source -> second frequency component.

- For $\bar{\mathbf{v}}_0^A = -(20\,\mathrm{m/s})\,\hat{\mathbf{z}}$ and $\bar{\mathbf{v}}_0^B = (40\,\mathrm{m/s})\,\hat{\mathbf{z}}$ respectively, one gets $\delta\phi^A \delta\phi^B = 35\,\mathrm{rad}$.
- With $N=10^5$ detected atoms, a shot-noise-limited sensitivity at the 10^{-5} level can be reached in a hundred shots.
- Stanford's 10-m prototype or AION's 10-m fountain could also measure these time dilation effects with about two orders of magnitude lower sensitivity.



Atom source-Atom source Atom source

MAGIS-100



"gradiometric" configuration suppresses laser phase noise and effect of mirror vibrations

$$\delta\phi_A - \delta\phi_B = -2\left(\Delta E/\hbar\right)\left(\bar{\mathbf{v}}_0^A - \bar{\mathbf{v}}_0^B\right) \cdot \mathbf{g} \, T^2/c^2$$

Main systematic effects



- Effects suppressed when adding up the phase shift for reversed interferometers:
 - gravity gradients (co-location at 0.1 mm and 0.1 mm/s level \longrightarrow 10^{-4} relative uncertainty)
 - rotations
 - wave-front curvature & light shifts
- Pulse timing requirements: $\Delta T \lesssim 0.1 \,\mu \text{s}$ and $\delta \lesssim 300 \,\text{Hz} \longrightarrow 10^{-5}$ relative uncertainty
- Magnetic field inhomogeneities: $3 \text{ nT/m} \rightarrow 10^{-5}$ relative uncertainty
- Temperature gradients: $2 \text{ K} / 100 \text{ m} \longrightarrow \text{contribution at } 10^{-2} \text{ level}$

further improvement through characterization and post-correction



Comparison to quantum-clock interferometry

Quantum-clock interferometry



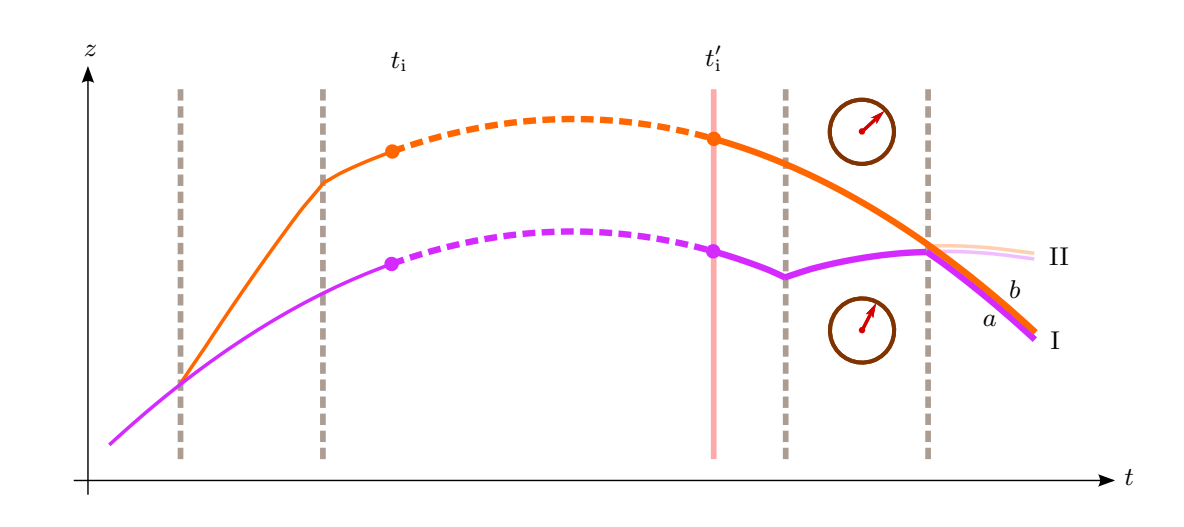
PHYSICAL REVIEW X 10, 021014 (2020)

Gravitational Redshift in Quantum-Clock Interferometry

Albert Roura

Quantum superposition of a single clock at two different heights

- Initialization pulse after the spatial superposition has been generated.
- Doubly differential measurement:
 - state-selective detection
 - compare different initialization times





Comparison with current proposal

 Quantum-clock interferometry: <u>single clock</u> in a delocalized quantum superposition of two wave packets experiencing different gravitational time dilation.

■ Current proposal: each atom interferometer acts as a *freely falling clock*; comparison between two independent clocks in the "gradiometric" configuration.



Conclusions



- Atom interferometers based on single-photon transitions can be used as freely falling clocks for time dilation measurements.
- Unprecedented measurement of relativistic time dilation in a local measurement with freely falling atoms.
- It could be implemented in MAGIS-100 with virtually no additional requirements.

A version with limited sensitivity could also be implemented in Stanford's 10-m prototype or AION's 10-m fountain.

Main challenge for achieving higher sensitivities
 temperature gradients.
 Further improvement through measurements of temperature profile and post-correction.



For further details:

Quantum Sci. Technol. 10 (2025) 025004

https://doi.org/10.1088/2058-9565/ad9e2e

Quantum Science and Technology

PAPER

Atom interferometer as a freely falling clock for time-dilation measurements

Albert Roura

German Aerospace Center (DLR), Institute of Quantum Technologies, Wilhelm-Runge-Straße 10, 89081 Ulm, Germany

E-mail: albert.roura@dlr.de

Keywords: atom interferometry, relativistic time dilation, gravitational and relativistic measurements, long-baseline facilities, single-photon clock transition



Thank you for your attention.



Project Q-GRAV